JOURNAL OF COMPUTATIONAL PHYSICS 59, 353–368 (1985)

Upwind Compact Finite Difference Schemes

I. CHRISTIE

Department of Mathematics, West Virginia University, Morgantown, West Virginia 26506

Received September 27, 1983; revised April 13, 1984

It was shown by Ciment, Leventhal, and Weinberg (*J. Comput. Phys.* **28** (1978), 135) that the standard compact finite difference scheme may break down in convection dominated problems. An upwinding of the method, which maintains the fourth order accuracy, is suggested and favorable numerical results are found for a number of test problems. © 1985 Academic Press, Inc.

1. INTRODUCTION

Compact finite differencing is a means of achieving high order discretisations of differential equations without an enlargement of the bandwidth of the resulting set of discrete equations. For example, for second-order problems in one space dimension, tridiagonal systems having fourth-order accuracy are produced. High accuracy coupled with easily solved systems are clearly most desirable properties of a numerical method.

In convection dominated problems, such as in fluid flow at moderate to large Reynolds numbers, standard numerical solutions often contain nonphysical oscillations. The removal of these oscillations involves either the use of an unrealistically small grid or a modification (upwinding) of the method.

One form of upwinding of compact methods was suggested by Berger, Solomon, Ciment, Leventhal, and Weinberg [2]. Their method which is of polynomial type ensures that a discrete maximum principle is satisfied. A method of exponential type developed by Leventhal [10] also ensures satisfaction of a discrete maximum principle. In both of these papers the methods were derived from a treatment of the whole differential equation as distinct from a second class of compact differencing methods which have been used by Hirsh [9] and more recently by Aubert and Deville [1], where derivatives are approximated individually to high order. In the Aubert and Deville paper, compact differencing is coupled with a transformation of coordinates in order to achieve better resolution of the boundary layer without an excessive number of mesh points. The latter methods do not require the linearisation of nonlinear problems necessary in the approaches of [2, 10]. However, no attempt has been made to upwind the method used by Hirsh and the purpose of this paper is to show the need for an upwinding and to present a way of achieving it.

0021-9991/85 $3.00

In Section 2 an analysis of the Hirsh scheme is given for a simple model problem and it shows that nonphysical oscillations may occur in the solution. Section 3 considers an upwinding of the compact method and a free parameter is introduced for which an optimal choice exists. Numerical results are presented which show the damping of the oscillations and also the important fact that the fourth-order accuracy is maintained at realistic mesh sizes. Finally, in Section 4, the upwind compact method is extended successfully to cover the cases of time dependent and nonlinear problems.

2. Compact Finite Differences

Consider the 1-dimensional model problem

$$u''(x) - Ku'(x) = 0, \qquad x \in [0, 1] \tag{1a}$$

$$u(0) = 1, \qquad u(1) = 0, \tag{1b}$$

where K is a positive constant. The theoretical solution is found easily to be

$$u(x) = \frac{e^{Kx} - e^{K}}{1 - e^{K}} \tag{2}$$

and, as K increases, a sharp boundary layer develops near $x = 1$. The same test problem has been used a number of times to construct upwind methods by Spalding [12] for finite differences and Christie, Griffiths, Mitchell, and Zienkiewicz [4] for finite elements. It was also used by Ciment, Leventhal and Weinberg [3] to investigate the spatial stability of compact methods.

Divide the unit interval into N equal subintervals $[(i-1)h, ih]$, $i = 1, 2, \ldots, N$, where the grid spacing is $h = 1/N$. Nonuniform grids may be used but they will not be considered here. Define the central, forward, and backward difference operators

$$D_0 U_i = \frac{U_{i+1} - U_{i-1}}{2h}, \quad D_+ U_i = \frac{U_{i+1} - U_i}{h}, \quad D_- U_i = \frac{U_i - U_{i-1}}{h}, \tag{3}$$

respectively. Then, first and second derivatives are approximated by F_i and S_i, respectively, where

$$F_i = \frac{D_0 U_i}{1 + \frac{h^2}{6} D_+ D_-} \tag{4}$$

$$S_i = \frac{D_+ D_- U_i}{1 + \frac{h^2}{12} D_+ D_-} \tag{5}$$

Multiplying across by the denominators in (4) and (5) and using the differential equation (1a) gives

$$\frac{1}{6}(F_{i+1}+4F_i+F_{i-1})=\frac{1}{2h}(U_{i+1}-U_{i-1}) \tag{6a}$$

$$\frac{1}{12}(S_{i+1}+10S_i+S_{i-1})=\frac{1}{h^2}(U_{i+1}-2U_i+U_{i-1}) \tag{6b}$$

$$S_i-KF_i=0. \tag{6c}$$

These equations hold for $i=1, 2,..., N-1$ and (6c) also holds at $i=0, N$. Therefore, additional boundary conditions are required. The system is tridiagonal and, if the U_i are given, it is very easily solved for the F_i and S_i. If the U_i are unknowns then ordering the unknowns as U_i, F_i, and S_i for each i gives a block tridiagonal system with 3×3 blocks. Taylor series expansions show that

$$F_i=U_i'-\frac{h^4}{180}U^{(5)}+\cdots, \tag{7}$$

$$S_i=U_i''-\frac{h^4}{240}U^{(6)}+\cdots, \tag{8}$$

and so (6) is a fourth-order tridiagonal system for the solution of (1).

To investigate further the nature of the solution (6), we can eliminate the F_i and S_i. This can only be done in the linear constant coefficient problem. Using (6c) to eliminate S_i from (6b) and then using (6a) gives

$$F_i=\frac{1}{2hL}[(2-L)U_{i+1}-4U_i+(2+L)U_{i-1}], \tag{9}$$

where $L=hK/2$. Substitution of (9) into (6a) leads to the five point formula in U_i,

$$(2-L)U_{i+2}+2(2-5L)U_{i+1}-12U_i+2(2+5L)U_{i-1}$$
$$+(2+L)U_{i-2}=0, \qquad i=2, 3,..., N-2. \tag{10}$$

It is interesting to note that formulas closely related to (10) are obtained from various high order Galerkin finite element methods discussed by de Boor [6], Douglas, Dupont, and Wheeler [7] and Rachford and Wheeler [11].

Although (10) leads to a five diagonal system, we stress that the implementation of the compact method involves tridiagonal or block tridiagonal matrices. It is convenient here to consider an analysis of the five point formulation.

The quartic characteristic polynomial of (10) gives the four roots $\lambda=1$, λ_1, λ_2 and λ_3. The latter three roots solve the cubic equation

$$(2-L)\lambda^3+(6-11L)\lambda^2-(6+11L)\lambda-(2+L)=0 \tag{11}$$

which was found by Ciment, Leventhal, and Weinberg [3]. The theoretical solution of (10) therefore is

$$U_i = A + B\lambda_1^i + C\lambda_2^i + D\lambda_3^i, \tag{12}$$

where A, B, C, and D are constants. The presence of a negative root of (11) in Eq. (12) will result in an oscillatory solution.

To see which values of L produce a negative root of (11) notice first that all three roots λ_1, λ_2, and λ_3 are real. In fact, on introducing

$$\lambda = \frac{1}{2-L}\left(\mu - 2 + \frac{11}{3}L\right) \qquad (L \neq 2), \tag{13}$$

(11) reduces to the form

$$\mu^3 + 3H\mu + G = 0, \tag{14}$$

where

$$G = \tfrac{8}{27}(108 - 324L + 279L^2 - 200L^3) \tag{15}$$

$$H = \tfrac{-4}{9}(18 - 21L + 22L^2). \tag{16}$$

Tartaglia's condition (see Durell and Robson [8]) for real roots of (14) and hence (11) is that $G^2 + 4H^3 < 0$. Here we have that

$$G^2 + 4H^3 = \tfrac{-64}{729}(L-2)^2(32L^4 + 39L^2 + 36) \tag{17}$$

is negative and so (11) does have three real roots.

Differentiation of (11) shows that its turning points $\lambda = \alpha$, β can be found from

$$3(2-L)\lambda^2 + 2(6-11L)\lambda - (6+11L) = 0. \tag{18}$$

Denoting the product and sum of the roots by p and s, respectively, we have for $L \neq 2$ that

$$p = -\frac{1}{3}\left(\frac{6+11L}{2-L}\right) \tag{19}$$

$$s = -\frac{2}{3}\left(\frac{6-11L}{2-L}\right). \tag{20}$$

If $L = 2$ then (11) has two negative roots. If $L > 2$ then $s < 0$ so that $\alpha < 0$ and/or $\beta < 0$. Since α and β are the turning points of the cubic (11) and all the roots are real, there must be a negative root. Similarly if $0 < L < 2$ then $p < 0$ so that $\alpha < 0$ or $\beta < 0$ and again there is a negative root. Therefore, for any possible L, this shows that the compact scheme (6) will contain oscillations.

TABLE I

Solution of Compact Scheme (6) Using (21): $h = 0.1$, $c = 0.5$

	$L=1$		$L=5$	
Node	Exact	Numerical	Exact	Numerical
0	1	1	1	1
1	1	1	1	1.673
2	1	1	1	0.911
3	1	1	1	1.832
4	1	1	1	0.710
5	1	0.999	1	2.077
6	1	1.002	1	0.411
7	0.988	0.933	1	2.441
8	0.982	0.990	1	−0.029
9	0.865	0.838	1	2.936
10	0	0	0	0

Using a different argument to the above, the ever presence of oscillatory solutions for a similar problem was noted by Ciment, Leventhal, and Weinberg [3]. To remove the oscillatory behavior they used an operator compact implicit method of polynomial type. It was pointed out in [3] that the oscillations may be insignificant at lower values of K in which case the nonupwind compact scheme can be applied without difficulty. Our goal however, is the removal or damping of the oscillations inherent in the method at larger values of K and fixed h and we restrict interest to this situation.

In Table I some numerical results are presented to show the extent of the oscillations contained in (6) as K increases. Additional boundary relations were obtained from

$$U_i - U_{i+1} + h[cF_i + (1-c)F_{i+1}] + \frac{h^2}{2}\left[\left(c-\frac{1}{3}\right)S_i + \left(c-\frac{2}{3}\right)S_{i+1}\right] + \frac{h^4}{12}\left(c-\frac{1}{2}\right)U^{(4)} = 0 \qquad (21)$$

which was also used by Hirsh. The formula is fifth order when $c = 0.5$ and fourth order otherwise. A fixed grid size of $h = 0.1$ was chosen and the solution was calculated at $K = 20$ and 100, corresponding to $L = 1$ and 5, respectively. The higher order ($c = 0.5$) boundary relations were used. Comparison with the exact values shows the large oscillations at $K = 100$ which swamp the solution completely.

3. Upwind Compact Finite Differences

In this section an attempt is made to damp out the oscillations inherent in the standard compact differences. The second derivatives are found again from Eq. (5) but for the first derivatives a modification of the form

$$F_i = \frac{(1-\gamma)\, D_0 + \gamma D_-}{1 + (h^2/6)\, D_+ D_-}\, U_i \tag{22}$$

is made to introduce the free parameter γ. The new system of equations to be solved consists of (6b) and (6c) together with

$$\frac{1}{6}(F_{i+1} + 4F_i + F_{i-1}) = \frac{1}{2h}((1-\gamma)\, U_{i+1} + 2\gamma U_i - (1+\gamma)\, U_{i-1}). \tag{23}$$

Taylor series expansions give the truncation error as

$$F_i = U_i' - \frac{h^4}{180}\, U^{(5)} - \frac{\gamma h}{2}\, U'' + \cdots, \tag{24}$$

and so $\gamma = O(h^3)$ is necessary to maintain the fourth-order accuracy. Notice that the choice $\gamma = 1$ which gives a backward difference on the numerator of (22) leads to a low-order approximation in (24).

Eliminating S_i and F_i between (6b), (6c), and (23) gives the five point formula in U_i

$$\begin{aligned}[2-(1-\gamma)L]\, U_{i+2} + 2[2-(5-4\gamma)L]\, U_{i+1} - 2[6+9\gamma L]\, U_i \\ + 2[2+(5+4\gamma)L]\, U_{i-1} + [2+(1+\gamma)L]\, U_{i-2} = 0.\end{aligned} \tag{25}$$

The characteristic equation gives $\lambda = 1$ and the other three roots come from the cubic

$$\begin{aligned}[2-(1-\gamma)L]\, \lambda^3 + [6-(11-9\gamma)L]\, \lambda^2 \\ - [6+(11+9\gamma)L]\lambda - [2+(1+\gamma)L] = 0.\end{aligned} \tag{26}$$

Choosing γ so that a root of (26) is e^{2L}, which is a root of the exact characteristic equation gives

$$\gamma = \gamma_{\text{opt}} = \coth L - \frac{2}{L}\left[\frac{e^{2L} + 4 + e^{-2L}}{e^{2L} + 10 + e^{-2L}}\right] \tag{27}$$

and a series expansion shows that for this optimal value

$$\gamma_{\text{opt}} = \frac{-L^3}{45} - \frac{977}{37800} L^5 - \cdots. \tag{28}$$

Thus $\gamma = O(h^3)$ for fixed K.

TABLE II

Numerical Solution of (1) Using the Upwind Compact Method

	$L=1$			$L=5$			$L=20$		
Node	Exact	$c=\frac{1}{2}$	$c=\frac{5}{6}$	Exact	$c=\frac{1}{2}$	$c=\frac{5}{6}$	Exact	$c=\frac{1}{2}$	$c=\frac{5}{6}$
0	1	1	1	1	1	1	1	1	1
1	1	1	1	1	1	1	1	1	1
2	1	1	1	1	1	1	1	1	1
3	1	1	1.001	1	1	1	1	1	1
4	1	1	0.998	1	1	1	1	1	1
5	1	0.999	1.004	1	1.002	1	1	1	1
6	1	1.001	0.990	1	0.994	1	1	1	1
7	0.997	0.993	1.019	1	1.024	1.002	1	1.001	1
8	0.982	0.990	0.941	1	0.907	0.992	1	0.992	1
9	0.865	0.839	0.990	1	1.363	1.031	1	1.056	1.002
10	0	0	0	0	0	0	0	0	0
Maximum error		0.024	0.125		0.363	0.031		0.056	0.002

Numerical results for the upwind compact method are shown in Table II and the additional boundary data is again provided by (21). A comparison with Table I shows a clear reduction in the oscillations. With $c = 0.5$, however, fairly substantial errors still appear when $L = 5$ and this suggests that an upwinding of the boundary relations should also be carried out. To accomplish this, observe that when S_i is eliminated from (6b), (6c), and (23),

$$F_i = \frac{1}{2hL}\left[(2-(1-\gamma)L)\,U_{i+1} - (4+2\gamma L)\,U_i + (2+(1+\gamma)L)\,U_{i-1}\right]. \tag{29}$$

If U_i is the exact solution (2) and $\gamma = \gamma_{\text{opt}}$ then

$$F_i = \frac{6(e^L - e^{-L})^2\, e^{2Li}}{hL(1-e^K)(e^{2L}+10+e^{-2L})}. \tag{30}$$

Substitution of (30) and (6c) into (21) shows that

$$c = c_{\text{opt}} = \frac{(6-5L)\,e^{2L} - (6+8L) + Le^{-2L}}{6((1-L)\,e^L - (1+L)\,e^{-L})(e^L - e^{-L})}. \tag{31}$$

With the values $\gamma = \gamma_{\text{opt}}$ and $c = c_{\text{opt}}$ the upwind compact scheme is exact. For large L, $c_{\text{opt}} \to \frac{5}{6}$ and results for this value, also presented in Table II, show an improvement over those for $c = \frac{1}{2}$ at the larger values of L.

Figure 1 shows the graphs of γ_{opt} and c_{opt} as L increases. Taking limits as $L \to 0$ in γ_{opt} and c_{opt} gives the respective values of 0 and $\frac{1}{2}$. For L slightly positive the graph of γ_{opt} is just negative. This reiterates the conclusion of Ciment, Leventhal, and Weinberg [3] that there exists a threshold below which upwinding is

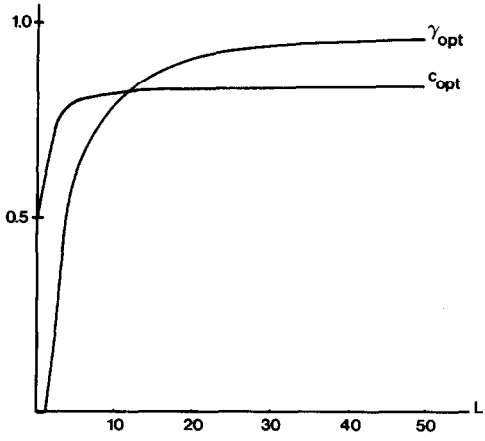

FIG. 1. Graphs of γ_{opt} and c_{opt} versus L.

TABLE III

Convergence Rates for Maximum Error in F

	$\gamma = 0$		$\gamma = \gamma_{opt}$	
N	Error	Rate	Error	Rate
10	6.53E–2		6.46E–2	
20	5.47E–3	3.58	5.23E–3	3.63
40	4.00E–4	3.77	3.74E–4	3.81
80	2.71E–5	3.88	2.51E–5	3.90
160	1.76E–6	3.94	1.62E–6	3.95
320	1.13E–7	3.96	1.03E–7	3.97

unnecessary. This is further seen in Table II, where for $L = 1$ the oscillations are mild.

In Table III the rate of convergence of the maximum error in F_i is computed as the grid size is successively halved. Assuming $E_h = kh^p$ and $E_{h/2} = k(h/2)^p$ are two successive maximum errors then the rate p is estimated from

$$p = \frac{1}{\ln 2} \ln(E_h / E_{h/2}). \tag{32}$$

The nonupwind scheme $\gamma = 0$ is compared to that using γ_{opt} with the values $K = 10$ and $c = 0.5$. The computed rates agree closely with the theoretical order of the method. It should also be emphasized that the fourth-order convergence is achieved for *realistic values of h* in the sense that an excessive number of mesh points is not required to maintain the accuracy. The results could probably be improved by the use of a variable grid in the boundary layer region such as that in [1].

4. Time Dependent Problems

The extension of the upwind compact method to time dependent problems is straightforward. The first test problem to be solved was

$$v u_{xx} - K u_x = u_t, \qquad (x, t) \in [0, 1] \times [0, \infty) \tag{33a}$$

$$\begin{aligned} u(0, t) &= 1, \qquad u(1, t) = 0, \qquad t > 0, \\ u(x, 0) &= 1, \qquad 0 \leqslant x < 1, \qquad u(1, 0) = 0, \end{aligned} \tag{33b}$$

where v and K are positive constants. Equation (33a) becomes

$$v S_i^* - K F_i^* = \frac{U_i^{n+1} - U_i^n}{\Delta t}, \qquad n = 0, 1, \ldots, \tag{34}$$

TABLE IV

Compact Solution of $vu_{xx} - Ku_x = u_t$: $h = 0.1$, $\Delta t = 0.01$, $t = 0.5$

	$L=1$		$L=5$	
Node	$\gamma = \gamma_{opt}$	$\gamma = 0$	$\gamma = \gamma_{opt}$	$\gamma = 0$
0	1	1	1	1
1	1	1	1	1.667
2	1	1	1	0.917
3	1	1	1	1.837
4	1	1	1.001	0.713
5	1	0.999	0.999	2.066
6	1	1.002	1.001	0.407
7	0.998	0.993	1	2.462
8	0.982	0.990	1	−0.048
9	0.865	0.838	1	2.940
10	0	0	0	0

where Δt is the time step and $t = n\,\Delta t$. The superscript * in (34) denotes the time level at which F_i and S_i are to be evaluated. Equations (23) and (6b) complete the compact system and U_i, F_i, S_i are also evaluated at *. If $* = n$ then the explicit system is very easy to solve. However as Hirsh pointed out, this scheme has severe stability restrictions. We made use of the Crank–Nicolson method ($* = n + \frac{1}{2}$) in which case

$$F_i^* = \tfrac{1}{2}(F_i^{n+1} + F_i^n)$$

$$S_i^* = \tfrac{1}{2}(S_i^{n+1} + S_i^n)$$

and the system is unconditionally stable with second-order accuracy in time.

If the unknowns are ordered as U_i^{n+1}, F_i^*, and S_i^* then the banded system of equations is block tridiagonal and each block is 3×3. A simpler system with 2×2 blocks can be produced by using (34) to eliminate one of the unknowns. This smaller system was used for the computations.

In Table IV results are presented for (33). The grid size was $h = 0.1$ and the time step in the Crank–Nicolson time discretisation was $\Delta t = 0.01$. The solution is shown after 100 time steps, at $t = 0.5$. The additional boundary relations were found from (21). With $\gamma = 0$ (no upwinding), $c = \frac{1}{2}$ and with $\gamma = \gamma_{opt}$, $c = c_{opt}$. In formulas (27) and (31) we used $L = hK/2v$. The viscosity was fixed at $v = 1$ and two values $K = 20$ and $K = 100$ were chosen. At the lower value of L, the standard ($\gamma = 0$) compact solution is well behaved and only very mild oscillations appear. At $L = 5$, however, the results contain large oscillations. The use of the upwind scheme damps out the oscillations.

The convergence rates given in Table V were obtained from

$$p = \frac{1}{\ln 2} \ln \left[\frac{U_h - U_{h/2}}{U_{h/2} - U_{h/4}} \right] \tag{35}$$

TABLE V

Convergence Rates for $vu_{xx} - Ku_x = u_t$: $K = 10$, $v = 1$, $t = 0.4$, $\gamma = \gamma_{opt}$

N	Δt	Steps	$u(0.9)$	Rate
80	6.25E-3	64	0.63214510669621	
160	1.5625E-3	256	0.63214488298773	3.94
320	3.90625E-4	1024	0.63214486844268	3.93
640	9.765625E-5	4096	0.63214486749075	

where $U_h = U + kh^p$ and U is the exact value. The grid size was halved twice to obtain three successive approximations at a point and U and k were eliminated to give (35). Values of $K = 10$ and $v = 1$ were chosen and the solutions were compared at $x = 0.9$. The mesh was reduced according to $\Delta t = 40h^2$ and since the Crank–Nicolson method is second order in time the expected rate is $p = 4$. Close agreement with this value was found numerically and similar results to those in Table V were also found when $\gamma = 0$.

The second problem to be solved consisted of the nonlinear Burgers' equation

$$vu_{xx} - uu_x = u_t \qquad (x, t) \in [0, 1] \times [0, \infty) \tag{36a}$$

along with the boundary conditions and initial condition

$$\begin{aligned} u(0, t) &= u(1, t) = 0, \qquad t > 0, \\ u(x, 0) &= \sin \pi x, \qquad 0 \leqslant x \leqslant \pi. \end{aligned} \tag{36b}$$

This problem was studied by Cole [5] who predicted the appearance of a sharp boundary layer near $x = 1$ as the viscosity v decreases.

The Crank–Nicolson discretisation of the upwind compact system leads to a nonlinear set of equations given by (23), (6b), and

$$vS_i^* - U_i^* F_i^* = \frac{U_i^{n+1} - U_i^n}{\Delta t}, \qquad n = 0, 1, \ldots, \tag{37}$$

where $* = n + \frac{1}{2}$ and in (23), (6b), the terms U_i, F_i, S_i are also computed at $n + \frac{1}{2}$. Equation (37) can be used to eliminate one of the unknowns U_i^*, F_i^*, S_i^*, and the result is a nonlinear system of equations. These were solved by Newton iteration in which the Jacobian turned out to be block tridiagonal with 2×2 blocks.

Table VI shows the computed convergence rates from formula (35) at $x = 0.9$ and $t = 0.5$. To use γ_{opt} a value of L had to be selected and $L = h/2v$ was found to work well. The viscosity was $v = 0.1$ and the grid was reduced according to $\Delta t = 5h^2$. Again there is close agreement with the predicted rate. A smaller value $v = 0.01$ was also selected but produced results for which the convergence was not monotone so that formula (35) could not be used.

TABLE VI

Convergence Rates for Burgers' Equation: $\nu = 0.1$, $t = 0.5$, $\gamma = \gamma_{opt}$

N	Δt	Steps	$U(0.9)$	Rate
10	5.0*E*–2	10	0.311000087	
20	1.25*E*–2	40	0.309451004	3.97
40	3.125*E*–3	160	0.309352226	4.00
80	7.8125*E*–4	640	0.309346064	4.00
160	1.953125*E*–4	2560	0.309345679	

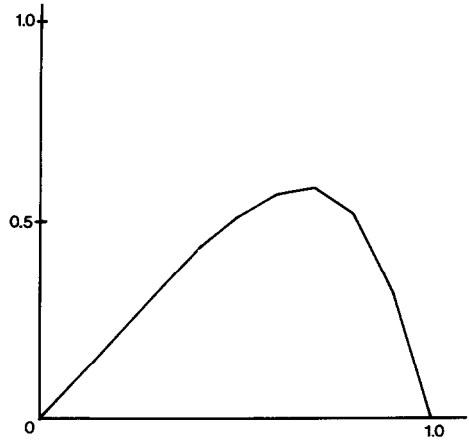

FIG. 2. Burgers' equation, $t = 0.5$, $\nu = 0.1$. Upwind and non-upwind solutions.

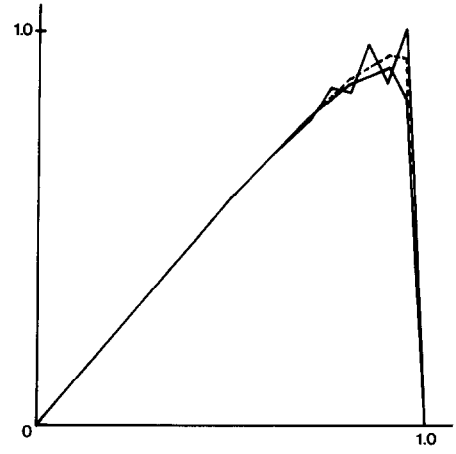

FIG. 3. Burgers' equation, $t = 0.5$, $\nu = 0.01$. Broken line denotes the upwind solution with $N = 160$. Non-upwind (oscillatory) and upwind solutions were calculated with $N = 20$.

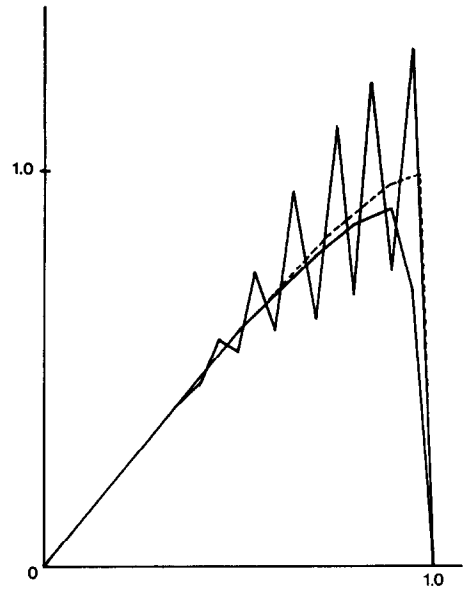

FIG. 4. Burgers' equation, $t = 0.5$, $\nu = 0.001$. $N = 160$ upwind (broken line), $N = 20$ non-upwind (large oscillations) and upwind.

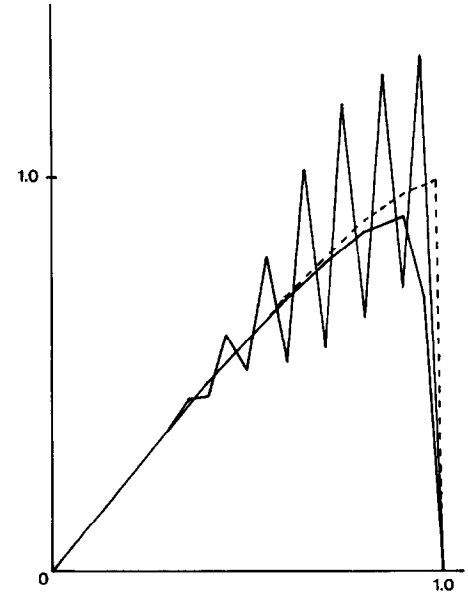

FIG. 5. Burgers' equation, $t = 0.5$, $\nu = 0.0001$. $N = 160$ upwind (broken line), $N = 20$ non-upwind (large oscillations) and upwind.

A series of numerical calculations were performed to compare the upwind and nonupwind compact schemes when ν is decreased from 0.1 to 0.0001. The results are presented at $t = 0.5$ in Figs. 2–5. No simple analytical solution exists for this problem so an accurate solution was also calculated for comparison using $N = 160$ in the upwind scheme. The additional boundary information was found satisfactorily when a value of $c = 0.5$ was used throughout. For unknown reasons c_{opt} led to poor convergence in Newton's method and was not used here. This was in contrast to the linear problems solved previously, where c_{opt} gave more favorable results than $c = \frac{1}{2}$. In all calculations the mesh ratio was $\Delta t/h^2 = 5$.

In Fig. 2 the viscosity is $\nu = 0.1$ which turns out to be an easy case and all the methods perform well. A single curve is shown and both upwind and nonupwind methods gave this for $N = 20, 160$.

In Fig. 3 we have $\nu = 0.01$. The upwind and nonupwind solutions were found with $N = 20$. An oscillation has appeared in the nonupwind results and this has been effectively smoothed out by the upwinding. The broken line denotes an accurate solution which was found from the upwind solution with $N = 160$.

Reducing the viscosity to $\nu = 0.001$ gives the results graphed in Fig. 4 and those for $\nu = 0.0001$ are shown in Fig. 5. Again $N = 20$ for the upwind and nonupwind schemes and $N = 160$ provides the accurate solution for comparison denoted by the broken line. In each of these figures the nonupwind solution produces a huge

TABLE VII

Solution of Burgers' Equation at $t = 0.5$, $\nu = 0.0001$, $\Delta t = 5h^2$

	Upwind (γ_{opt})		Non-upwind	
x	$N = 20$	$N = 160$	$N = 20$	$N = 160$
0.9	0.891	0.959	0.721	0.820
		0.962		1.187
		0.965		0.818
		0.968		1.212
		0.971		0.817
		0.973		1.237
		0.976		0.814
		0.978		1.264
0.95	0.682	0.980	1.306	0.811
		0.981		1.291
		0.983		0.807
		0.984		1.320
		0.985		0.803
		0.985		1.349
		0.988		0.798
		0.761		1.379
1.0	0	0	0	0

oscillation which is damped by the upwinding. At the lower values of v the upwinding has overdamped the solution in the boundary layer region.

The actual numerical values for $v = 0.0001$ are given in Table VII at the boundary layer. These values were used in Fig. 5. The nonupwind solution contains large oscillations even at $N = 160$. Despite the loss of accuracy in the boundary layer the upwinding has achieved its goal of damping the oscillations and no doubt with a variable grid there would be a better resolution of the boundary layer.

5. Conclusion

The standard compact finite difference method as used by Hirsh is unsuitable in certain convection dominated problems. An upwinding of this method has been suggested and it has been demonstrated that the large nonphysical oscillations which occur with the standard compact scheme can be damped out. The overdamping of the solution in the boundary layer suggests that in practice a variable mesh approach such as done by Aubert and Deville may be useful. One consideration here is that a variable mesh in the boundary layer would mean small h values and, since $\gamma = O(h^3)$, the possible elimination of the upwinding.

Work is underway to apply the upwind compact scheme to 2-dimensional flow problems. Of significance in these cases will be the choice of upwinding parameters. The work of Hirsh showed for the driven cavity problem that greatly increased accuracy is obtained by the standard compact method with far fewer mesh points than a second-order method. It remains to be seen whether the upwinding is capable of the improvement in 2-dimensional problems which it gave for the 1-dimensional case.

Acknowledgments

The author is grateful to the National Research Institute for Mathematical Sciences of the CSIR in Pretoria, South Africa where the bulk of this work was carried out. Particular thanks are due to Drs. Duncan Martin and Dirk Laurie for arranging a visiting position from May to August 1983.

References

1. X. Aubert and M. Deville, *J. Comput. Phys.* **49** (1983), 490.
2. A. E. Berger, J. M. Solomon, M. Ciment, S. Leventhal, and B. C. Weinberg, *Math. Comp.* **35** (1980), 695.
3. M. Ciment, S. H. Leventhal, and B. C. Weinberg, *J. Comput. Phys.* **28** (1978), 135.
4. I. Christie, D. F. Griffiths, A. R. Mitchell, and O. C. Zienkiewicz, *Int. J. Numer. Methods Eng.* **10** (1976), 1389.
5. J. D. Cole, *Q. Appl. Math.* **9** (1951), 225.
6. C. R. de Boor, "The Method of Projections as Applied to the Numerical Solution of Two Point Boundary Value Problems Using Cubic Splines," Ph.D. thesis, University of Michigan, 1966.

7. J. DOUGLAS, T. DUPONT, AND M. F. WHEELER, H^1-Galerkin methods for the Laplace and heat equations, *in* "Math. Aspects of Finite Elements" (C. de Boor, Ed.), Academic Press, New York, 1974.
8. C. V. DURELL AND A. ROBSON, "Advanced Algebra," Vols. II, III, Bell, London, 1937.
9. R. S. HIRSH, *J. Comput. Phys.* **19** (1975), 90.
10. S. H. LEVENTHAL, *J. Comput. Phys.* **46**, No. 1 (1982), 138.
11. H. H. RACHFORD AND M. F. WHEELER, An H^{-1}-Galerkin procedure for the two point boundary value problem, *in* "Math. Aspects of Finite Elements" (C. de Boor, Ed.), Academic Press, New York, 1974.
12. D. B. SPALDING, *Int. J. Numer. Methods Eng.* **4** (1972), 552.